Aerosol and Air Quality Research, 15: 410–425, 2015

ISSN: 1680-8584 print / 2071-1409 online
doi: 10.4209/aaqr.2014.08.0172

Chemical Composition of Fine and Coarse Aerosol Particles in the Central Mediterranean Area during Dust and Non-Dust Conditions

Antonella Malaguti*, Mihaela Mircea, Teresa M.G. La Torretta, Chiara Telloli, Ettore Petralia, Milena Stracquadanio, Massimo Berico

ENEA - National Agency for New Technologies, Energy and Sustainable Economic Development, via Martiri di Monte Sole 4, 40129 Bologna, Italy

ABSTRACT

A two-month field campaign was carried out from May to June 2010 at a remote site (Trisaia ENEA Research Centre) in the Southern Italy aiming to identify and quantify the changes of aerosol chemical composition in the presence of Saharan dust. The 24-hr PM_{10} and $PM_{2.5}$ filter samples were analyzed by mass, carbonaceous species, inorganic ions and elemental composition. Saharan dust transport events were identified with two approaches: one recommended by EC (2011) and one based on indicators derived from measurements. Three indicators were used: $PM_{2.5}/PM_{10}$ mass concentrations ratio, Ca/Al ratio and Al concentration. Based on these criteria, four Saharan dust transport events were identified, but only one had elevated dust concentration and leaded to an exceedance of the European short-term (24 hour) limit value of 50 μg/m^3 for PM_{10} (June 16th). The comparison of chemical composition of fine and coarse aerosol fractions during dust and non-dust conditions shows that the presence of dust increases NH_4 and $nssSO_4$ concentrations in the fine fraction and NO_3 and $nssSO_4$ concentrations in the coarse fraction. OC and EC concentrations also increase in the fine fraction during dust transport. The uptake of primary and secondary species, inorganic and organic, by dust particles changes their composition and, thus, their properties and this may have implications for human health and climate change.

Keywords: Saharan dust; Fine and coarse chemical composition; Central Mediterranean (Southern Italy).

INTRODUCTION

Mineral dust particles originating in the Sahara desert are frequently transported over the whole Mediterranean area.

An eleven years study of Saharan dust outbreaks in the whole Mediterranean basin revealed that the dust transport paths have a marked seasonal behavior (Pey *et al.*, 2013). The western Mediterranean area is more subjected to dust intrusions during the summer season while in the eastern part dust events are more frequent during the autumn-spring period. The central area results to be a transitional region, with frequent occurrence of African dust outbreaks in summer over the central Italy and in autumn-spring over Sicily. Thus, southern part of Italy is affected by Saharan dust intrusions in all seasons.

These events may lead to substantial increase of aerosol mass concentrations (Perez *et al.*, 2008; Pederzoli *et al.*, 2010; Remoundaki *et al.*, 2013, Marconi *et al.*, 2014), leading to exceedances of the PM_{10} daily limit value (50 μg/m^3) established by the European Directive 2008/50/EC on air quality (EC, 2008). The experimental studies were mainly devoted to the knowledge of chemical composition of coarse aerosol fraction since this contributes most to the increase in PM_{10} mass concentrations. Recently, Sajani *et al.* (2012) shown that the dust is also a substantial part of fine aerosol fraction which penetrates in the deepest part of the lung, therefore, its role in aerosol effects on human health has to be investigated. Moreover, dust particles interact with gases and other aerosol species contributing to an increase of aerosol mass and to a change in their chemical composition (Aymoz *et al.*, 2004).

The chemical characterization of atmospheric particles is a common approach to quantify the primary or secondary contribution from natural or anthropogenic sources (Kocak *et al.*, 2007; Rinaldi *et al.*, 2007; Perrino *et al.*, 2009; Salvador *et al.*, 2012). Three main classes of aerosol compounds, carbonaceous, inorganic and elements, are usually analyzed.

The carbonaceous aerosol is one of the most important ubiquitous materials in the atmosphere and comprises organic carbon (OC), elemental carbon (EC) and carbonaceous carbon (CC). OC can be attributed to either natural and anthropogenic sources, EC is a pollutant emitted from combustion of fossil fuels or biomass combustion and CC is present in soils and rocks, and is related to natural sources.

* Corresponding author.
Tel.: 39-051-6098090; Fax: 39-051-6098675
E-mail address: antonella.malaguti@enea.it

In regions around Mediterranean coasts, the water-soluble ionic species accounted for a significant portion of the total mass both in fine and coarse fractions (Nicolas *et al.*, 2009). Primary inorganic ions such as Na^+, Cl^-, Ca^{2+} and Mg^{2+}, are mainly emitted from natural sources (soil and water surfaces) and secondary inorganic aerosol (SIA) such as NO_3^-, SO_4^{2-} and NH_4^+ are produced by chemical reactions in the atmosphere from anthropogenic gaseous precursors (NO_x, SO_2 and NH_3).

Wind-driven suspension of particles from surface soils and desert gives rise to natural dust contribution to aerosol (Viana *et al.*, 2008). The main elements present in dust are Al, Si, Ca and Fe and according to Kocak *et al.* (2012) and Marconi *et al.* (2014), Al concentrations greater than 1 μg/m^3 and Ca/Al ratio values indicate the presence of Saharan dust.

Several studies have quantified chemical composition of aerosol in the Mediterranean area during Saharan dust events (Querol *et al.*, 2001, Gómez-Amo *et al.*, 2011, Kocak *et al.*, 2012, Öztürk *et al.*, 2012; Bougiatioti *et al.*, 2013).

In Italy, chemical characterization of particulate matter during Saharan dust outbreaks was carried out mainly on PM_{10} fraction (Perrino *et al.*, 2009; Gómez-Amo *et al.*, 2011; Nava *et al.*, 2012; Marconi *et al.*, 2014), but information about the chemical composition of fine fraction, in the southern part of Italy is not available.

This study shows the daily mineral dust concentrations in the coarse and fine aerosol fractions and identifies the related changes in chemical composition at a rural background site, located at ENEA Research Centre of Trisaia, Southern Italy. The experimental campaign was carried out for two months, from the beginning of May to the end of June 2010 (Malaguti *et al.*, 2013). While Malaguti *et al.* (2013) had analyzed the diurnal variation of carbonaceous aerosols and its sources using semi-continuous measurements of organic (OC) and elemental carbon (EC), here the daily aerosol samples were analyzed for determination of mass concentrations of PM_{10} and $PM_{2.5}$, carbonaceous aerosol fraction, water-soluble ionic species and trace elements.

Special focus is given to the estimation of mineral dust mass concentrations and to the analysis of the changes in chemical composition induced by dust.

METHODS

Sampling

The field campaign was carried out at Trisaia ENEA Research Centre (Italy) (40°09′58.23″N–16°38′25.95″E, 25 m altitude) from May 3rd to June 30th 2010. The site is located in the South of Italy (Fig. 1(a)), 4 km away from the Ionian Sea, in an area without industrial plants and large cities, close to the end of the Sinni river valley (Fig. 1(b)). Other information on site description and meteorological conditions during the campaign can be found in Malaguti *et al.* (2013). Based on AERONET data (http://www.esrl.noaa.gov/gmd/obop/mlo/programs/coop/nasa/aeronet/aeronet.html), MODIS maps (http://modis-atmos.gsfc.nasa.gov/MOD04_L2/index.html) and air mass back trajectories (Fig. 2) computed with NOAA HYSPLIT model (http://ready.arl.noaa.gov/HYSPLIT.php), four Saharan dust events were identified, three in May (3–5, 10–12, 26–28) and one in June (11–18). The aerosol was sampled with size-selective $PM_{2.5}$ and PM_{10} sampling inlets, simultaneously on polytetrafluoroethylene (PTFE) membranes and quartz fiber filters, in order to allow gravimetric analyses and inorganic soluble ion concentrations, carbonaceous aerosol concentrations and multi element analysis. Samples were collected over 24 hours, with start time at 00:01 UTC.

Sample collections for gravimetric analysis were performed with a Hydra Dual Channel Sampler (FAI-Instruments) equipped with a cooling system for the sampled filters unloader to assure samples stability. The flow rate on each independent channel was 2.30 ± 0.05 m^3/h, complying with European Standards EN12341:1998 and EN14907:2005 for PM_{10} and $PM_{2.5}$ standard sampling. Particles were collected on PTFE membrane filters (Pall TEFLO W/RING pore size 1.0 μm Ø47 mm R2PL047).

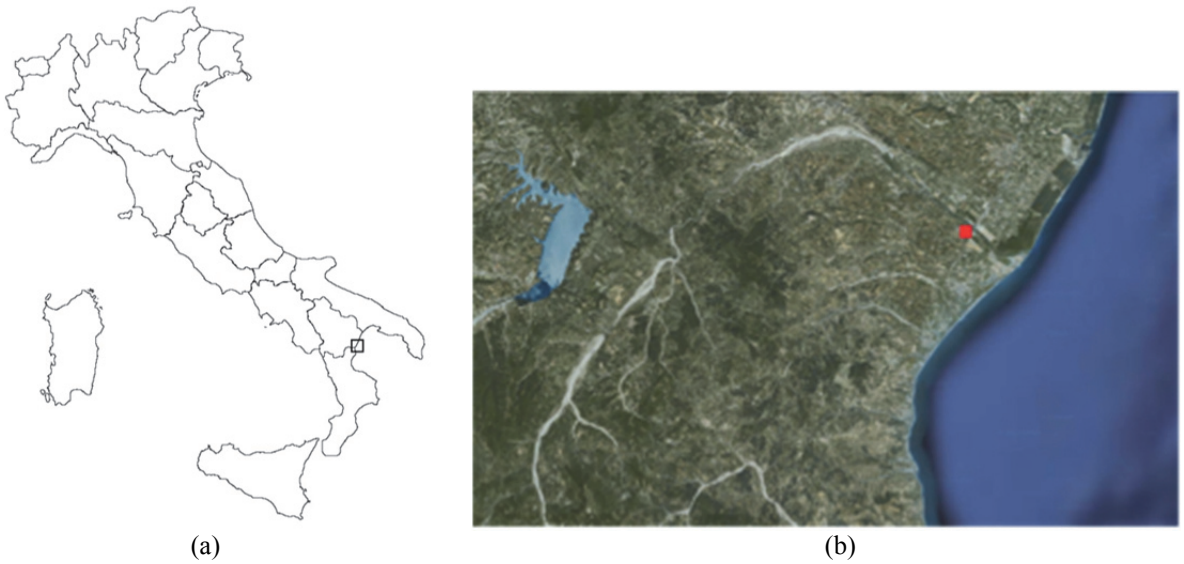

(a) (b)

Fig. 1. (a) Map of Italy and (b) map of Sinni River Valley with squares representing the sampling area.

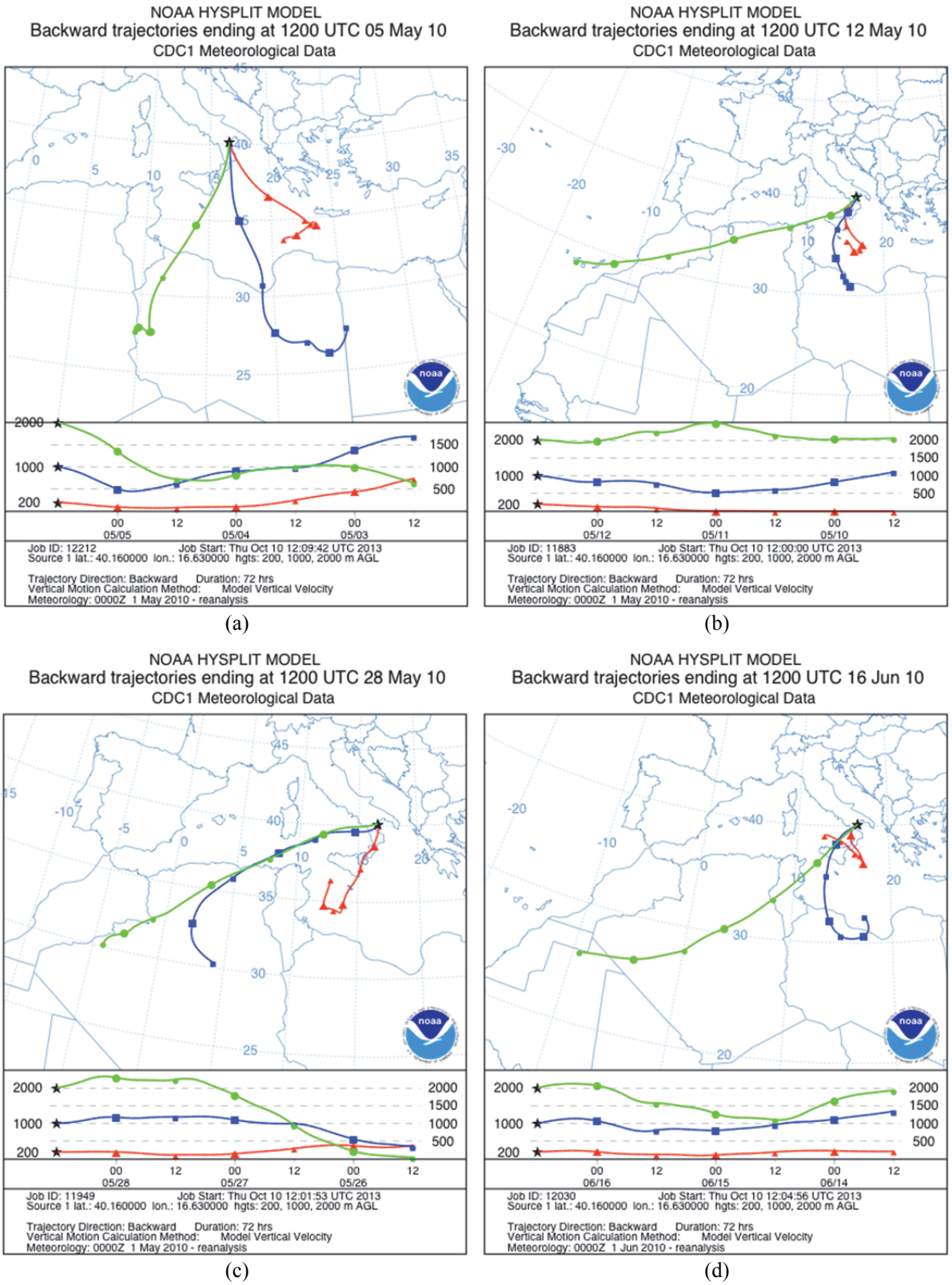

Fig. 2. 72-h backward trajectories of air masses sampled (a) from May 3rd to May 5th, (b) from May 10th to May 12th, (c) from May 26th to May 28th, (d) from May 14th to May 16th.

$PM_{2.5}$ and PM_{10} sample collections for inorganic soluble ion analysis were performed with two atmospheric particles monitor samplers (FAI SWAM 5A Monitor). The flow rate was 2.30 ± 0.05 m^3/h. Particles were collected on quartz fibre filters (Pall 2500-QUAT-UP Ø47 mm) and preserved at –20°C.

$PM_{2.5}$ and PM_{10} samples for carbonaceous fraction and multi-element analysis were collected on quartz micro-fibre filters (Pall 2500-QAT-UP 7204 8 × 10 in) using high volume samplers with flow rates of 68 ± 1 m^3/h (Dust samplers High Volume Graseby Andersen and Tisch-Analitica respectively for PM_{10} and $PM_{2.5}$ sampling). The filters were pre-fired at 850°C for three hours before use and stored in baked aluminum foil. After collection the filters were punched in five sub-samplers (80 mm diameter), placed in plastic Petri dishes and stored in a freezer (at –20°C).

The equivalence of Hydra and FAI SWAM samples has been confirmed by the values of regression coefficients (R^2) and slopes obtained for $PM_{2.5}$ (R^2 = 0.80; slope = 0.96) and PM_{10} (R^2 = 0.94; slope = 1.01) measurements performed with gravimetric and beta attenuation methods, respectively.

The same method was applied for the high volume and FAI SWAM samplers for sodium and calcium measured on $PM_{2.5}$ and PM_{10} filters. The $PM_{2.5}$ and PM_{10} regression coefficients of determination and slopes were also close to 1 (Table 1).

Gravimetric Measurements and Chemical Analyses

PM_{10} and $PM_{2.5}$ masses were determined by weighing the filters before and after the sampling using an electronic balance (Mettler Toledo, model AX205, sensitivity 0.01 mg). All filters were conditioned for 48 hours prior to weighing at a relative humidity of 50 ± 5% and temperature of 20 ± 1°C, as required by EN12341:1998 and EN14907:2005. The measurement uncertainty was 10% and 5% for $PM_{2.5}$ and PM_{10}, respectively.

Table 1. Interspecies correlations. Regression coefficients of determination (R^2) greater than 0, 50 (statistically significant: $p > 0.05$) are reported.

parametrs	slope	r^2
PM_{10} SWAM vs. PM_{10} Hydra	1.01	0.94
$PM_{2.5}$ SWAM vs. $PM_{2.5}$ Hydra	0.96	0.80
PM_{10} - Na HV vs. Na SWAM	1.06	0.91
PM_{10} - Ca HV vs. Ca SWAM	0.91	0.93
$PM_{2.5}$ - Na HV vs. Na SWAM	1.11	0.85
$PM_{2.5}$ - Ca HV vs. Ca SWAM	0.98	0.92
PM_{10} MD method 4(a) vs. method 3	1.21	0.94
$PM_{2.5}$ MD method 4(b) vs. method 3	0.76	0.91
PM_{10} MD method 5 vs. method 3	1.04	0.94
$PM_{2.5}$ MD method 5 vs. method 3	0.53	0.90
$PM_{2.5}$ EC vs. OC	0.18	0.51
$PM_{2.5}$ WSOC vs. OC	0.59	0.75
PM_{10} Mg vs. Na	0.15	0.76
$PM_{2.5}$ SO_4 vs. NH_4	1.09	0.96
PM_{10} NO_3 vs. (Na + Ca)exc	0.92	0.83
PM_{10} ∑+ vs. ∑–	1.17	0.89
$PM_{2.5}$ ∑+ vs. ∑–	1.16	0.94
PM_{10} nssCa vs. Al	0.79	0.88
PM_{10} Fe vs. Al	0.52	0.95
PM_{10} Ti vs. Al	0.08	0.94
PM_{10} nssMg vs. Al	0.16	0.80
PM_{10} Fe vs. nssCa	0.60	0.91
PM_{10} Ti vs. nssCa	0.01	0.92
PM_{10} nssMg vs. nssCa	0.18	0.75
PM_{10} nssMg vs. Fe	0.52	0.76
PM_{10} nssMg vs. Ti	3.63	0.68
PM_{10} Ti vs. Fe	0.15	0.93

OC and EC mass concentrations were determined with a Sunset Laboratory Dual-Optical Carbonaceous Analyzer (Sunset Laboratory). The analyses were performed with the EUSAAR_2 thermal optical transmittance protocol (Cavalli *et al.*, 2010) since this protocol has been specifically developed for rural background samples. The limits of detection (LOD) for OC and EC were calculated as three times the standard deviation of laboratory blank concentrations (3σ), thus the LOD for OC and EC were 0.048 μgC/cm^2 and 0.0002 μgC/cm^2, respectively, with an uncertainty estimated of 5%. Blank correction was performed by subtracting the blank average value to the sample filters values. The handling and sampling positive OC artefacts (Kirchstetter *et al.*, 2001) were estimated on the basis of the OC concentrations measured on the field blanks and back up filters respectively (Malmone *et al.*, 2011). The values obtained both for handling and sampling artefacts were not subtracted from the reported OC concentration as indicated in PD CEN/TR 16243:2011. The field blanks were collected approximately every 20 field samples, the OC concentration ranged from 0.343–0.462 μgC/cm^2. The OC handling artefact represents 15% of OC concentrations on average. The back-up filters were collected on 10% of sampling days, the OC concentration ranged from 0.30 to 0.60 μgC/m^3 both for PM_{10} and $PM_{2.5}$ and the OC sampling artefact represents 15–17% of OC concentrations on average. The presence of CC may cause positive artefacts to the OC concentration evolving during the He-mode with EUSAAR-2 protocol (Cavalli *et al.*, 2010). Therefore, the CC (the CO_3^{2-} mass concentration expressed as μgC/m^3) was estimated from Ca^{2+} and Mg^{2+} mass concentration (Querol *et al.*, 2001; PD CEN/TR 16243:2011) obtained by IC and ICP-MS analyses, respectively. The CO_3^{2-} mass concentrations in PM_{10} for the dust period were estimated with two methods: one based on Ca^{2+} and Mg^{2+} concentrations and the other based on the thermal optical sunset OCEC analyzer software.

Method 1 is based on the Eq. (1) (Querol *et al.*, 2001):

$$1.5\text{nssCa} + 2.5\text{nssMg} = CO_3^{2-} \quad (1)$$

while method 2 estimated the carbonate carbon (CC) using the thermal optical sunset OCEC analyser software following the indications reported in "Ambient air quality – Guide for the measurement of elemental carbon (EC) and organic carbon (OC) deposited on filters"- Annex C – procedure 5 (PD CEN/TR 16243:2011). The CC was further multiplied by a factor 5 in order to obtain the CO_3^{2-} mass concentration.

In order to avoid the overestimation of particulate organic matter (POM) concentrations, the CC concentrations (expressed as μgC/m^3) have been subtracted from the OC concentrations and the corrected OC values have been used for both fine and coarse POM estimations.

Water-soluble organic carbon (WSOC) was extracted by hand-shaking for 5 min with 20 mL of Milli-Q (Millipore gradient A10) water from a 9 cm^2 sample piece punched

from the quartz filters. The extract was filtered through a PTFE syringe filter (pore size 0.2 μm) and analyzed using a Shimadzu TOC-5000A Total Carbon Analyzer equipped with a high sensitive catalyst (Viana *et al.*, 2006). LOD for WSOC, calculated as three times the standard deviation (3σ) of the laboratory blank concentrations, was 0.13 μgC/m^3 and the estimated uncertainty was 5%. Water insoluble organic carbon (WISOC) concentrations were calculated as the difference between OC and WSOC.

The multi-element analysis was carried out using an ICP-MS, X Series spectrometer, collision/reaction cell CCT^{ED} (Thermo Electron Corporation).

The aerosol samples collected on quartz fiber filters (Pall 2500-QAT-UP 7204) were extracted using acid digestion in a hotplate open system with HF, HNO_3 and H_2O_2. Field blanks were systematically below LOD. LOD value were calculated as three times the standard deviation (3σ) of blanks: 0.001 μg/m^3 for Mg, K and Ti, 0.003 μg/m^3 for Al, 0.004 μg/m^3 for Ca and Fe, and the estimated uncertainty ranged from 5% to 10%.

Anions (Cl^-, NO_3^-, SO_4^{2-}) and cations (Na^+, K^+, NH_4^+, Ca^{2+}, Mg^{2+}) were analyzed by ion chromatography (IC) after ultrasonic extraction with 10 mL of deionized water for 30 min and filtration through 0.20 μm Dionex filters. The analysis of anions were performed using a Dionex DX-120, the separation column was an AS9HC 250 × 4 mm with Na_2CO_3 8 mM + $NaHCO_3$ 1.5 mM as eluent running at 1 mL/min. The analysis of cations were performed using a Dionex 500, the separation column was a CS12A 250 × 4 mm with methane sulfonic 20 mM as eluent running at 1 mL/min. The injection volume was 100 μL. LOD values, calculated as three times the standard deviation (3σ) of blanks in μg/m^3 were 0.015 for Cl^-, 0.010 for NO_3^-, 0.133 for SO_4^{2-}, 0.012 for Na^+, 0.012 for NH_4^+, 0.024 for K^+, 0.027 for Ca^{2+} and 0.01 for Mg, the estimated uncertainty was 1% for NO_3^-, SO_4^{2-}, Ca^{2+}, Mg, NH_4^+, 10% for Cl^-, Na^+, and 14% for K^+.

Calculation of Sea-salt and Dust

The main components of salt mass dissolved in seawater are: sodium (Na^+), chloride (Cl^-), magnesium (Mg^{2+}), calcium (Ca^{2+}), potassium (K^+) and sulphate (SO_4^{2-}). The sea-salt (SS) fraction of SO_4^{2-}, K^+ and Ca^{2+} were calculated from the measured Na^+ concentrations and the standard seawater composition (Seinfeld and Pandis, 1998; Putaud *et al.*, 2004; Radhi *et al.*, 2010). The non-sea-salt (nss) fraction of SO_4^{2-}, K^+ and Ca^{2+} were calculated by subtracting the sea-salt fractions from their measured concentrations. Finally, the sea salt (SS) mass concentration was calculated using the following equation (Putaud *et al.*, 2010):

$$[SS] = Cl^- + Mg^{2+} + Na^+ [1 + (SO_4^{2-}/Na^+)_{sw} + (Ca^{2+}/Na^+)_{sw} + (K^+/Na^+)_{sw}] \quad (2)$$

The concentration of mineral dust matter in the atmosphere can be estimated with different approaches. The traditional approaches use formulas based on dust elemental data (Pettijohn, 1975; Querol *et al.*, 2001; Perez *et al.*, 2008; Querol *et al.*, 2009), while other approaches are based on Ca^{2+} data (Putaud *et al.*, 2004; Guinot *et al.*, 2007). Due to the scarcity of these chemical data, a statistical methodology for PM_{10} data was recently developed and applied (Escudero *et al.*, 2007; Pey *et al.*, 2013).

The mineral dust (MD) mass concentration was estimated with traditional approach based on analyzed dust elemental data. MD mass concentrations in fine and coarse aerosol samples were calculated as the sum of the main crustal elements (Perez *et al.*, 2008; Querol *et al.*, 2009; Putaud *et al.*, 2010) using a modified equation reported by Putaud *et al.* (2010):

$$[MD] = Al_2O_3 + SiO_2 + CO_3^{2-} + nssCa^{2+} + nssMg^{2+} + 1.42[Fe] + 1.94[Ti] \quad (3)$$

Since the silica and carbonate were not measured, the concentrations of SiO_2 and CO_3^{2-} were indirectly determined from Ca^{2+}, Mg^{2+} and Al concentrations, using experimental equations reported by Querol *et al.* (2001):

$$1.5nssCa + 2.5nssMg = CO_3^{2-} \quad (1)$$

$$3Al_2O_3 = SiO_2 \quad (1a)$$

The concentrations of Ca^{2+} and Mg^{2+} represent the non-sea-salt fraction. The factors used for Fe and Ti were reported by Pettijohn, (1975).

In addition to the above method, other two approaches were tested for estimating MD, during the dust period, both based on Ca^{2+} concentrations and represented by the following equations:

$$MD = Ca^{2+}/0.055 \text{ for } PM_{10} \quad (4a)$$

$$MD = Ca^{2+}/0.039 \text{ for } PM_{2.5} \quad (4b)$$

$$MD = 15.0 \times nssCa^{2+}, \text{ Saharan dust period} \quad (5)$$

The Eqs. 4(a) and 4(b) are based on method reported by Guinot *et al.* (2007), where the mass of total dust material is estimated from soluble Ca^{2+} ion concentration using a conversion factor. The conversion factors for PM_{10} and $PM_{2.5}$ are calculated as the slope of the linear regression of Ca^{2+} versus missing mass (unidentified matter, UM, here) and are shown in Figs. 3(a) and 3(b). UM was estimated as the difference between the weighted aerosol mass and the chemical retrieved mass. The feasibility of this approach for the evaluation of dust in PM_{10} and $PM_{2.5}$ was supported by the good correlations between Ca^{2+} and UM.

The Eq. (5) based on correlations between $nssCa^{2+}$ and mineral dust estimated from a campaign carried out at Mt. Cimone (Italy) from 4 June to 4 July 2000 (Putaud *et al.*, 2004) was considered for comparison.

Chemical Mass Closure for Coarse and Fine Aerosol Fractions

Aerosol chemical mass closure was performed for each daily sample. For reconstructing fine ($PM_{2.5}$) and coarse

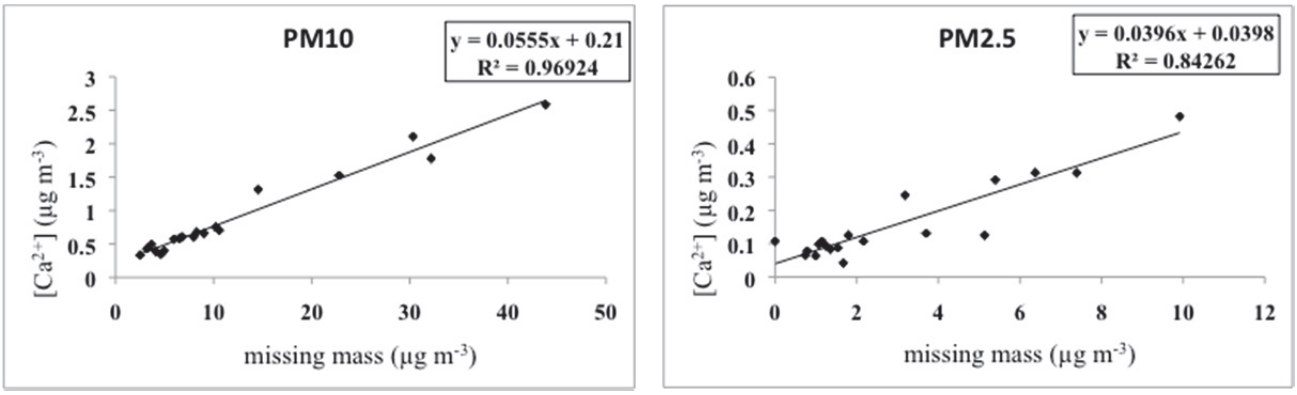

(a) (b)

Fig. 3. Correlation between the Ca^{2+} concentrations and the missing mass for PM_{10} (a) and $PM_{2.5}$ (b) during the dust periods (19 samples).

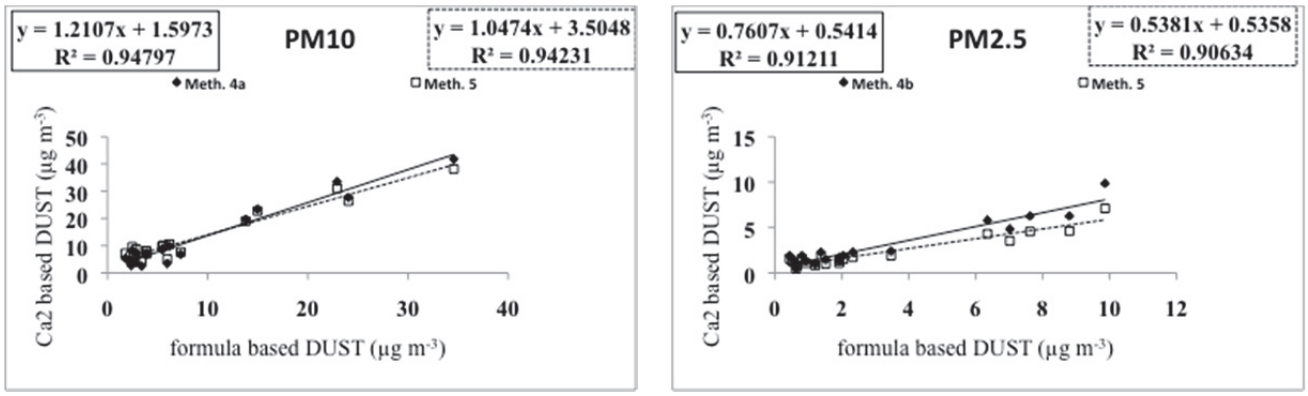

(a) (b)

Fig. 4. Linear regressions between MD concentrations estimated with formula based method and Ca^{2+} based methods for PM_{10} (a) and $PM_{2.5}$ (b) during the dust periods (19 samples).

($PM_{10-2.5}$) gravimetric mass, the chemical components were divided into five classes as follows: secondary inorganic ions (NO_3^-, $nssSO_4^{2-}$ and NH_4^+) (SIA), SS estimated using the Eq. (2), MD estimated using the Eq. (3), EC and POM estimated by multiplying OC with a conversion factor (CF), which is the ratio of the average molecular mass to the carbon mass for the organic aerosol. CF ranges from 1.4 to 2.1 for urban and rural/background aerosol respectively (Guinot *et al.*, 2007; Perez *et al.*, 2008; Flament *et al.*, 2011). The highest CF is related to the high percentage of WSOC (> 40%) reported for rural sites in Europe (Turpin and Lim, 2001; Kiss *et al.*, 2002). Based on the high percentage of WSOC with respect to OC (58.4%) and the location of site in a rural area, a CF of 1.9 has been used for the estimation of POM for both fine and coarse fractions. Unidentified matter (UM) represents the difference between the gravimetric mass and the sum of the five components (SIA, SS, MD, EC, POM).

RESULTS AND DISCUSSION

Quantification of Carbonate Carbon (CC) and Mineral Dust

The mean mass concentrations of CO_3^{2-} calculated from Ca and Mg (Eq. (1)) and from the thermal optical sunset OCEC analyzer software (method 2) are similar in spite of the fact that the two methods are based on different assumptions. The mean mass concentrations of CO_3^{2-} were 1.69 (Eq. (1)) and 1.92 (method 2) µg/m^3 for all dust events, and 2.45 (Eq. (1)) and 2.37 (method 2) µg/m^3 for the main dust event. It can be noted that the difference due to the chosen method is more important for all dust events (+13%) than for the main dust event (–3%.).

Figs. 4(a) and 4(b) shows the linear regressions between the MD concentrations obtained by the traditional approach (Eq. (3)) and Ca^{2+} based methods (Eqs. (4) and (5)). It can be noted that Eq. (4) which use the on-site measurements gives better estimations than Eq. (5) for both PM_{10} (Fig. 4(a)) and $PM_{2.5}$ (Fig. 4(b)).

PM_{10} and $PM_{2.5}$ Concentrations

Table 2 shows the statistics of daily concentrations of PM_{10} and $PM_{2.5}$ for the whole campaign. PM_{10} and $PM_{2.5}$ daily concentrations vary from 8.03 to 60.88 and from 4.20 to 22.34 µg/m^3, respectively. [$PM_{2.5}$]/[PM_{10}] ratios vary between 0.32 and 0.79, where the lowest value corresponds to days with Saharan dust intrusions (Querol *et al.*, 2001; Kocak *et al.*, 2007).

Table 2. MIN, MAX, AVG and STD mass concentration for PM_{10}, $PM_{2.5}$, $PM_{10-2.5}$, $[PM_{2.5}]/[PM_{10}]$ ratio, EC, OC, CC, primary ions and secondary ions for $PM_{2.5}$ and $PM_{10-2.5}$ during the campaign. Fine fraction Mg^{2+} is not reported since its concentrations were below LOD.

	MIN μg/m³	MAX μg/m³	AVG μg/m³	STD μg/m³
PM_{10}	8.03	60.88	18.61	9.89
$PM_{2.5}$	4.20	22.34	10.98	3.99
$PM_{10-2.5}$	4.56	38.54	13.65	9.15
$PM_{2.5}/PM_{10}$	0.32	0.79	0.62	0.11
$EC(PM_{2.5})$	0.09	0.80	0.33	0.17
$EC(PM_{10})$	0.12	0.91	0.39	0.19
$OC(PM_{2.5})$	1.26	4.21	2.53	0.70
$OC(PM_{10})$	1.31	4.52	2.99	0.70
$CC(PM_{2.5})$	0.01	0.29	0.04	0.05
$CC(PM_{10})$	0.02	1.0	0.17	0.19
$Na(PM_{2.5})$	0.05	0.53	0.15	0.09
$Na(PM_{10-2.5})$	0.06	2.98	0.55	0.53
$Cl(PM_{2.5})$	0.02	0.12	0.05	0.02
$Cl(PM_{10-2.5})$	0.01	3.98	0.30	0.60
$K(PM_{2.5})$	0.04	0.31	0.12	0.07
$K(PM_{10-2.5})$	0.01	0.18	0.05	0.03
$Mg(PM_{10-2.5})$	0.01	0.24	0.06	0.05
$Ca(PM_{2.5})$	0.02	0.48	0.09	0.08
$Ca(PM_{10-2.5})$	0.04	2.10	0.37	0.40
$NO_3(PM_{2.5})$	0.04	0.24	0.09	0.04
$NO_3(PM_{10-2.5})$	0.05	2.05	0.64	0.51
$SO_4(PM_{2.5})$	0.55	7.21	2.83	1.71
$SO_4(PM_{10-2.5})$	0.09	2.03	0.56	0.44
$NH_4(PM_{2.5})$	0.24	2.42	1.09	0.58

Fig. 5 shows the temporal variability of PM_{10} and $PM_{2.5}$ mean daily concentrations and $[PM_{2.5}]/[PM_{10}]$ ratios; the four periods with Saharan dust transport are identified by the rectangles. It can be noted that the European short-term (24 hour) limit value of 50 μg/m³ for PM_{10}, requested by the EU air quality standards (Directive 2008/50/EC), was exceeded only once on June 16th (60.88 μg/m³) and the highest levels of both PM_{10} and $PM_{2.5}$ concentrations were observed between June 14th and 18th (average PM_{10} was 36 μg/m³ and average $[PM_{2.5}]/[PM_{10}]$ ratio was 0.49), during an intense dust transport event from Sahara. The other three dust episodes identified in May were characterized by average PM_{10} concentrations of 26 μg/m³, 20 μg/m³ and 24 μg/m³ and average $[PM_{2.5}]/[PM_{10}]$ ratios of 0.54, 0.61 and 0.57. In the absence of dust, the average PM_{10} concentration was 14 μg/m³ and average $[PM_{2.5}]/[PM_{10}]$ ratio was 0.66.

Chemical Characterization

OC and EC are predominantly found in $PM_{2.5}$. On the opposite, CC fraction is mainly present in PM_{10} and its contribution to the atmospheric coarse mass concentrations may be significant in certain geographical locations such as Southern Europe and meteorological conditions such as African dust intrusion. WSOC concentration in $PM_{2.5}$ is generally a good proxy for secondary organic aerosol (SOA) (Miyzaki *et al.*, 2006; Sullivan and Weber, 2006; Kondo *et al.*, 2007) mainly in the absence of significant biomass burning emissions (Sullivan *et al.*, 2006; Weber *et al.*, 2007, Hennigan *et al.*, 2009). The fraction of WSOC in the OC is higher in summer than in other seasons, this is likely due to stronger photochemical oxidation of biogenic and anthropogenic precursors, forming oxygen containing functional groups (Viana *et al.*, 2006).

Table 2 shows the statistics of daily EC, OC and CC mass concentrations during the whole campaign. The average EC contained in daily PM_{10} and $PM_{2.5}$ range from 0.39 to 0.33 μg/m³ and the average OC contained in daily PM_{10} and $PM_{2.5}$ range from 2.99 to 2.53 μg/m³. The differences between the OC concentrations in PM_{10} and $PM_{2.5}$ may indicate an influence of coarse organic carbon sources such as primary bioaerosols (Minguillon *et al.*, 2012). CC daily mean concentrations, contained in PM_{10} and $PM_{2.5}$, samples range from 0.17 to 0.04 μg/m³. The daily averages of OC and EC mass concentrations in PM_{10} and $PM_{2.5}$ and of CC mass concentrations in PM_{10} are shown in Fig. 6. It can be noted that the CC mass concentration shows four peaks, corresponding to the four dust events, while OC and EC do

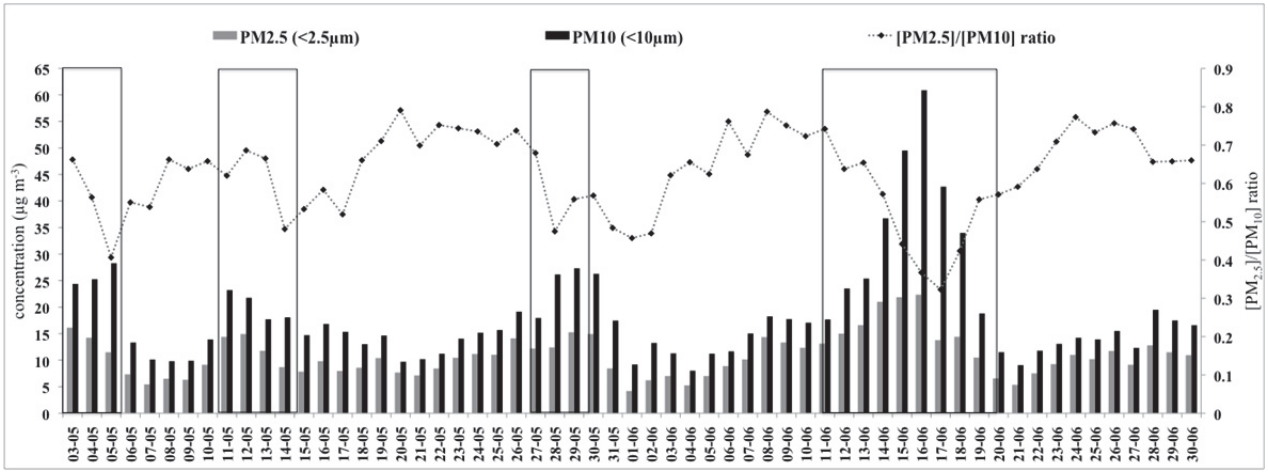

Fig. 5. Time pattern of PM_{10} and $PM_{2.5}$ mass concentrations and $[PM_{2.5}/[PM_{10}]$ ratios during the whole campaign. Periods with Saharan dust transport are identified by the rectangles.

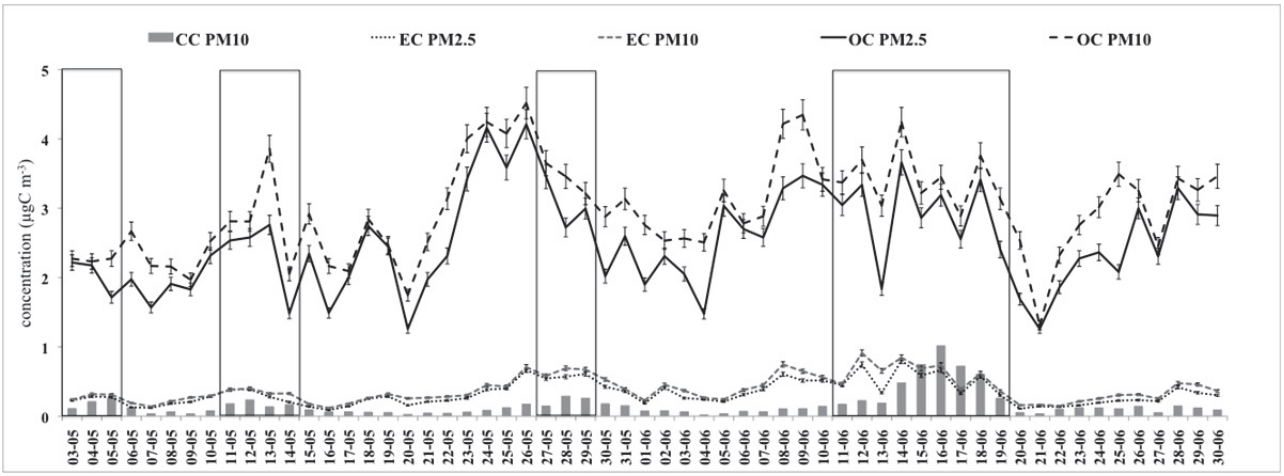

Fig. 6. Evolution of OC and EC mass concentrations (lines) in PM_{10} and $PM_{2.5}$ fractions and CC mass concentration (bars) in PM_{10} fraction during the whole campaign. Periods with Saharan dust transport are identified by the rectangles.

not show such behavior. Moreover, no different behavior is observed in the temporal trends of OC and EC contained in $PM_{2.5}$ and PM_{10} samples. The relative contributions of CC, EC and OC (WSOC + WISOC) to TC for the $PM_{2.5}$ were 1.5%, 11.6% and 86.9%, respectively. Moreover, WSOC accounted for 51.6% of the TC mass and for 58.4% of the total OC mass, these values are consistent with results reported for rural sites (Po Valley) (Decesari *et al.*, 2001) and for European non-urban environment (Pio *et al.*, 2007) respectively. The high contribution of WSOC to OC indicates the presence of secondary OC (aged or photo-chemically processed) (Theodosi *et al.*, 2010; Park and Cho, 2013). The EC and OC mass concentrations were mainly found in $PM_{2.5}$ (80% and 82% respectively), while the CC mass concentrations were found mainly in $PM_{10–2.5}$ (80%) as showed in Fig. 7.

The poor correlation between OC and EC mass concentrations ($R^2 = 0.51$) and the good correlation between WSOC and OC ($R^2 = 0.75$), (Table 1), suggest different sources for EC and OC. The EC was emitted by primary anthropogenic sources such as vehicular traffic for this site. On the contrary OC was mainly related to the SOA contribution, natural and anthropogenic, that was higher than the contribution of primary anthropogenic aerosol from traffic, as reported in Malaguti *et al.* (2013) and supported by Pio *et al.* (2007) for non-urban sites during summer in Europe.

All the primary ions derived from natural sources are mainly present in the PM_{10} fraction; among these, Na^+ and Cl^- are the main constituents of the sea salt, being considered the main marker elements of sea spray source; Ca^{2+} is a significant component of the soil dust and Mg^{2+} is grouped with the crustal elements in Southern Europe (Viana *et al.*, 2008); however, both Ca^{2+} and Mg^{2+} may have also marine origin. Mass concentrations and percentage contribution of primary ions to $PM_{10–2.5}$ and $PM_{2.5}$ are shown in Table 3 and Fig. 7, respectively. The K^+ daily mean and maxima concentrations in $PM_{10–2.5}$ and $PM_{2.5}$ vary from 0.01 to 0.18 and 0.4 to 0.31 μg/m^3 respectively. The amount of K^+ was higher in $PM_{2.5}$ than in $PM_{10–2.5}$ but the concentrations were both low since the period was characterized by the lack of fires in the area and at regional scale as shown by MODIS products (http://modis-land.gsfc.nasa.gov/fire.htm). Except for K^+, the other primary ions were mainly found in $PM_{10–2.5}$ (Fig. 7), as expected from the knowledge of their sources and formation mechanisms. Ca^{2+} mean and maximum concentrations in $PM_{10–2.5}$ were 0.37 and 2.10 μg/m^3. Mg^{2+} was detected only in $PM_{10–2.5}$ with daily mean and maximum concentrations values of 0.06 and 0.24 μg/m^3 respectively. Na^+ and Cl^- mean and maxima concentrations in $PM_{10–2.5}$ were 0.55 and 2.98 and 0.30 and 3.98 μg/m^3 respectively. Assuming that the sea salt tracer (Na^+) has a pure marine origin, the high correlation between Mg^{2+} and Na^+ (Table 1) indicated a common source for Mg^{2+} and Na^+ and the slope value of the regression line between Mg^{2+} and Na^+ (μequivalents/m^3) is relatively close to that reported for the seawater (0.12) confirming the sea spray origin of Mg^{2+}.

The mass ratio $[Cl^-]/[Na^+]$ in aerosols (average value 0.35 ± 0.28) is lower by a factor of 3.4 than the ratio in the seawater (1.18), indicating a deficit of Cl^- relatively to Na^+. This situation has been already observed at other remote coastal sites in the Mediterranean area, and is related to Cl^- depletion processes due to reaction of nitric and sulphuric acid with NaCl particles and subsequent loss of Cl^- through the volatilization of HCl (Sciare *et al.*, 2005; Koulouri *et al.*, 2008; Kishcha *et al.*, 2011).

Secondary inorganic ions are normally the major components of the $PM_{2.5}$ fraction, except nitrate whose distribution between fine and coarse aerosol fraction is influenced by location and meteorological conditions (Alastuey *et al.*, 2005; Sillanpaa *et al.*, 2006; Carbone *et al.*, 2010; Theodosi *et al.*, 2011).

Mass concentrations and percentage contribution of secondary ions to $PM_{10–2.5}$ and $PM_{2.5}$ fractions are showed in Table 2 and Fig. 7, respectively.

Daily mean and maximum concentrations of sulphate (SO_4^{2-}) in $PM_{10–2.5}$ and $PM_{2.5}$ fractions range between 0.56 and 2.03, and between 2.83 and 7.21 μg/m^3, respectively. Ammonium (NH_4^+) was present only in the fine fraction

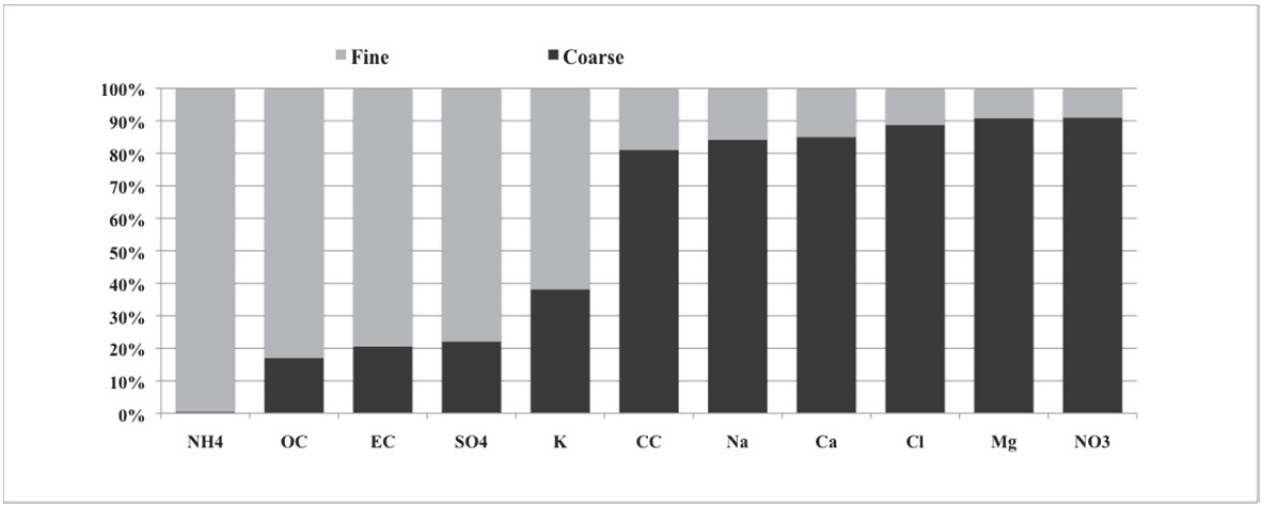

Fig. 7. Percentage contribution of OC, EC, CC and water-soluble ions to the fine and coarse fractions.

Table. 3. Mean concentrations of aerosol species in $PM_{2.5}$ and $PM_{10-2.5}$ for non-dust and dust periods.

	$PM_{2.5}$ non-dust	$PM_{2.5}$ dust	$PM_{10-2.5}$ non-dust	$PM_{10-2.5}$ dust
mass concentration ($\mu g/m^3$)	9.19	14.75	4.77	13.65
EC ($\mu gC/m^3$)	0.28	0.45	0.05	0.07
POM ($\mu g/m^3$)	4.63	4.93	0.76	0.49
MD ($\mu g/m^3$)	0.41	3.13	0.85	5.64
SS ($\mu g/m^3$)	0.22	0.34	0.75	1.78
SIA ($\mu g/m^3$)	3.05	5.93	0.64	1.95
NO_3^-	0.08	0.12	0.38	1.18
$nssSO_4^{2+}$	2.09	4.27	0.25	0.77
NH_4^+	0.88	1.54	0.01	0.01

and its daily mean and maximum concentrations correspond to 1.09 and 2.42 $\mu g/m^3$, respectively. The absence of ammonium in the coarse fraction may be explained by the fact that $NH_4NO_{3(s)}$ reacts with coarse NaCl resulting in the loss of gaseous NH_4Cl as observed also by Querol *et al.* (2004) and Nicolas *et al.* (2009). This reaction takes place during sampling and is more intense in PM_{10} which contain more sea-salt than in $PM_{2.5}$.

The mass concentration of sulphate and ammonium were mainly associated (ca. 80% and 100%, respectively) to $PM_{2.5}$ (Fig. 7). The strong correlation ($R^2 = 0.96$, slope = 1.1, in $\mu equivalents/m^3$) between SO_4^{2-} and NH_4^+ in $PM_{2.5}$ (Table 1) indicates that SO_4^{2-} was mainly present as $(NH_4)_2SO_4$.

Nitrate (NO_3^-) daily mean and maximum concentrations in $PM_{10-2.5}$ and $PM_{2.5}$ vary from 0.64 to 2.05 and from 0.09 to 0.24 $\mu g/m^3$, respectively. The low mass concentration of NO_3^- in the fine mode may be attributed to the formation of instable ammonium nitrate during warm season (Querol *et al.*, 2004; Sharma *et al.*, 2007; Theodosi *et al.*, 2011). In fact, the temperature was always above 20°C during the day (Malaguti *et al.*, 2013) favoring the well-known phenomenon of NH_4NO_3 evaporation from filters during sampling. This phenomenon is similar for Teflon and quartz filter as shown by Schaap *et al.* (2004).

The good correlation ($R^2 = 0.83$, in $\mu equivalents/m^3$) (Table 1), between NO_3^- and the sum of the excess of Na^+ with respect to the $[Cl^-]/[Na^+]$ marine ratio and of excess of Ca^{2+} relative to CO_3^{2-} ($Na^+ + Ca^{2+}$) exc in PM_{10}, indicates that NO_3^- was mainly present as $Ca(NO_3)_2$ and $NaNO_3$ and may be attributed to the reaction of gaseous HNO_3 with mineral species (i.e., $CaCO_3$) (Guinot *et al.*, 2007) and with sea salt (Alastuey *et al.*, 2005; Rinaldi *et al.*, 2007; Nicolas *et al.*, 2009). Moreover, the presence of $NaNO_3$ is supported by the low ratio value of $[Cl^-]/[Na^+]$ which may be due to the volatilization of Cl^- when the reaction between NaCl and HNO_3 (Alastuey *et al.*, 2005; Almeida *et al.*, 2006; Rinaldi *et al.*, 2007) takes place. The formation of nitrates could be also due to a sampling artefact produced by the reaction of gaseous pollutants or ammonium nitrate with dust and sea salt particles already collected in the filters (Querol *et al.*, 2004; Alastuey *et al.*, 2005; Nicolas *et al.*, 2009).

The ionic balance ($\sum+/\sum-$) from IC analysis was achieved both for PM_{10} ($\sum_{cations}(\mu eq/m^3) = 1.17\sum_{anions}$; $R^2 = 0.89$) and $PM_{2.5}$ ($\sum_{cations}(\mu eq/m^3) = 1.16\sum_{anions}$; $R^2 = 0.94$) (Table 1). The strong correlation between cations and anions both for PM_{10} and $PM_{2.5}$ indicated that the three anions and the four cations analyzed were the major ionic species. The slope values implied a deficiency in anions possibly due to CO_3^{2-} that has not been measured by IC; in this case CO_3^{2-} is expected to associate mainly with Ca^{2+}.

Concentrations of sodium, calcium and magnesium in PM_{10}, obtained with two different techniques, IC and ICP-MS methods, are shown in Fig. 8. The scatter plot (Fig. 8(a)) show a good correlation for both Na^+ ($R^2 = 0.91$; slope = 1.06)

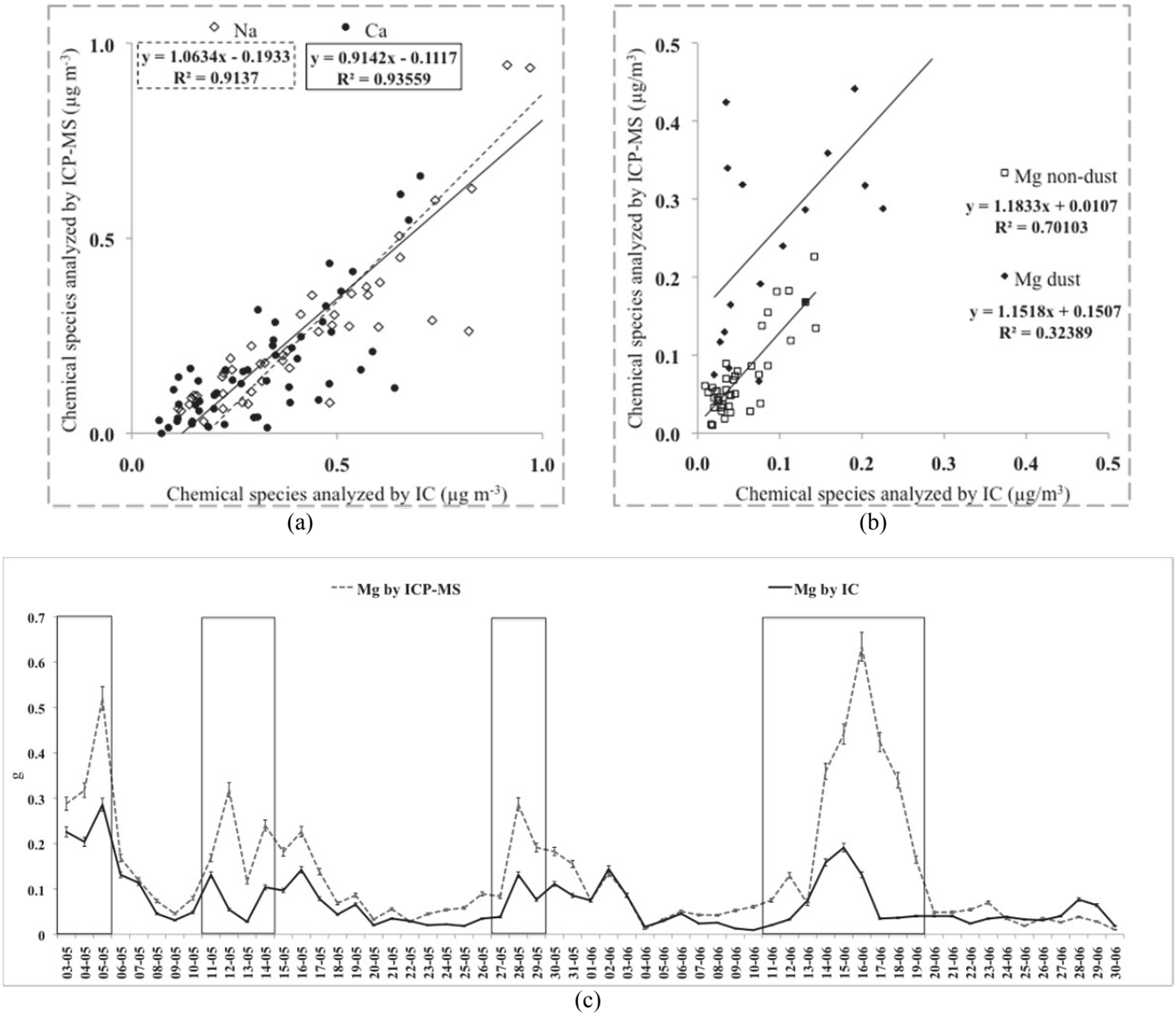

Fig. 8. Intercomparison of cations data obtained by IC and ICP-MS in the PM_{10} fraction, scatter plot of sodium and calcium data (a), scatter plot (b) and time pattern (c) of magnesium data for dust and non dust events, periods with Saharan dust transport are identified by the rectangles.

and Ca^{2+} (R^2 = 0.94; slope = 0.92) between the concentrations obtained by ICP-MS and the water soluble concentrations obtained by IC method, similarly to Koulouri *et al.* (2008). Based on these observations, it can be assumed that calcium obtained by IC represent the bulk calcium (Guinot *et al.*, 2007; Flament *et al.*, 2011). In the case of magnesium (Fig. 8(b)), during the dust and non-dust events were observed similar slope values (1.15 and 1.18 respectively) but different regression coefficient and intercept values (R^2: 0.32 and 0.70; intercept: 0.15 and 0.01), this may be due to insoluble Mg compounds, transported during dust events, that were detected only with the ICP-MS method. This hypothesis is supported by the fact that the Mg^{2+} concentrations in PM_{10} obtained by ICP-MS were higher than the corresponding concentrations obtained by IC during the days corresponding to dust events as showed in Fig. 8(c). Therefore, the estimation of mineral dust mass used the non-sea-salt magnesium obtained by ICP-MS and the $nssCa^{2+}$ obtained by IC.

The regression coefficients between the concentrations of major crustal elements in PM_{10} for the whole period are reported in Table 1; the highest values were obtained for Al, $nssCa^{2+}$, Fe, and Ti.

High concentrations of elements as Al and Fe or Ti are used as tracers of mineral dust events (Kocak *et al.*, 2007; Kocak *et al.*, 2012). Fig. 9 shows the daily concentrations of crustal elements recorded for PM_{10} (a) and $PM_{2.5}$ (b).

The concentrations show a similar temporal variability with peak concentrations in correspondence of the four dust episodes identified at the ground. The highest concentrations have been observed at ground level from June 14th to June 18th. According to Kocak *et al.* (2012) and Marconi *et al.* (2014), in the Mediterranean region, this mineral dust transport event can be classified as an intense dust episode since the aerosol Al concentration was higher than 1 µg/m^3

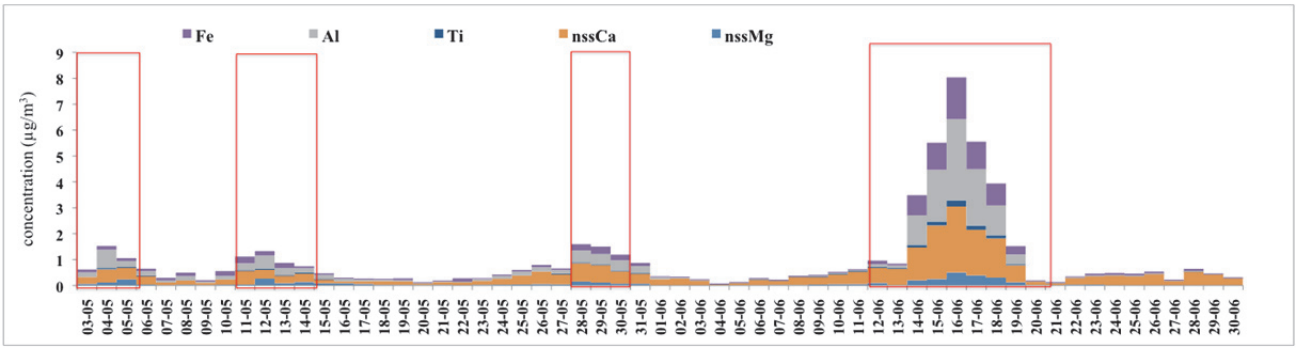

(a)

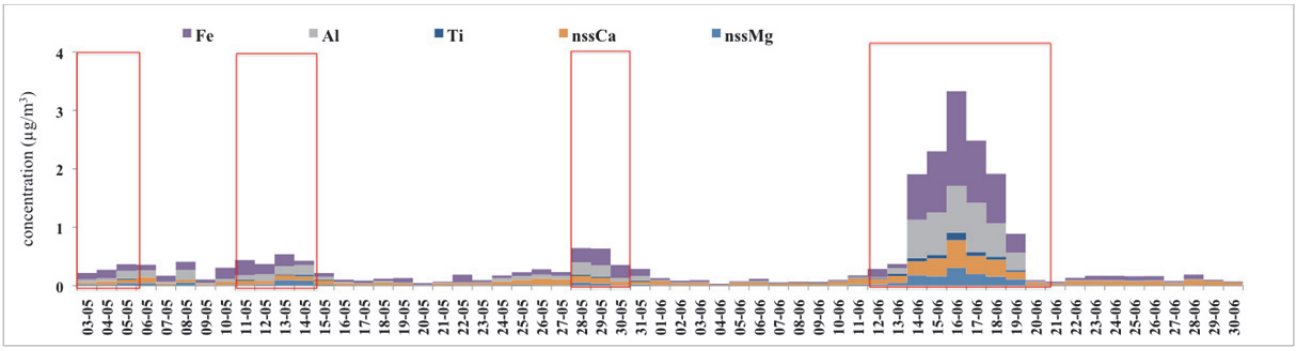

(b)

Fig. 9. Temporal variability of the daily concentrations of elements of crustal origin (Al, Fe, Ca, Ti, nssCa and nssMg) recorded for PM_{10} (a) and $PM_{2.5}$ (b). Periods with Saharan dust transport are identified by the rectangles.

and the Ca/Al ratio was in the range 1–2. The maximum Al concentration (3.13 µg/m^3) was recorded on June 16th with a MD mass concentration calculated of 34.57 µg/m^3. These values are similar to the values reported for crustal origin elements during intense dust events (Remoundaki *et al.*, 2013).

Influence of Dust Events on Chemical Composition of Aerosol and Mass Closure

The mean concentrations and percentage contribution of chemical species in $PM_{2.5}$ and $PM_{10–2.5}$ during non-dust and dust periods are shown in Table 3 and Fig. 10.

The $PM_{10–2.5}$ has been chosen for highlighting differences in aerosol characteristics between non-dust and dust periods.

As expected, the fine and coarse aerosol mass concentrations increased during dust period compared to non-dust period almost two times and three times, respectively. This was partly due to the increase of MD concentrations that was almost seven times higher than the values observed during non-dust period. The differences in EC and POM concentrations were small between dust and non-dust periods. SS advected from the sea area showed an increase of concentration more than two times during dust transport from Sahara, in particular in the coarse fraction. An important increase of SIA concentrations, both for fine and coarse aerosol fractions, was also observed during dust transport. This behavior is explained by the reactions between precursor inorganic gases and MD particle surfaces (Putaud *et al.*, 2004; Kocak *et al.*, 2007; Nicolas *et al.*, 2009). In the fine fraction, the enhancement of SIA may be related to the formation of $(NH_4)_2SO_4$ already observed during Saharan outbreaks in other European coastal sites (Nicolas *et al.*, 2009), while in the coarse fraction this enhancement is related to an higher formation of coarse $Ca(NO_3)_2$ (Putaud *et al.*, 2004; Guinot *et al.*, 2007; Nicolas *et al.*, 2009).

It can be noticed that in the presence of dust (MD), unidentified matter (UM) was reduced from 6.9% to zero in $PM_{2.5}$ (Figs. 10(a) and 10(b)) and was reduced by almost 10% in $PM_{10–2.5}$ (Figs. 10(c) and 10(d)). The former behavior is explained by the fact that dust is leading to a substantial increase of $PM_{2.5}$ and $PM_{10–2.5}$ mass concentrations followed by an important reduction of the percentage contribution of the UM which mass concentration remains almost unchanged during dust and non-dust event. The percentage of SIA increases in both fractions since their mass concentrations increase during the dust events (Table 3). In relative proportions, POM and SIA were the major compounds of $PM_{2.5}$. The contributions of EC and SS were relatively low, within a few percentages. Non-sea-salt sulphate was the dominant secondary anion during the whole campaign with a higher relative contribution during dust period than out of dust. The contributions of NH_4^+ and of NO_3^- are similar for both periods. The contribution of carbonaceous fraction (EC and POM), $nssSO_4^{2-}$ and NH_4^+ are consistent with data reported for other European rural sites (Carbone *et al.*, 2010; Bressi *et al.*, 2013). The dust enriched air mass contributed largely to the increase of $PM_{2.5}$ mass concentration, up to 21.2%, while during non-dust period the contribution was only 4.4%, similar to the values obtained by Bressi *et al.* (2013) for other European rural sites. Even though the

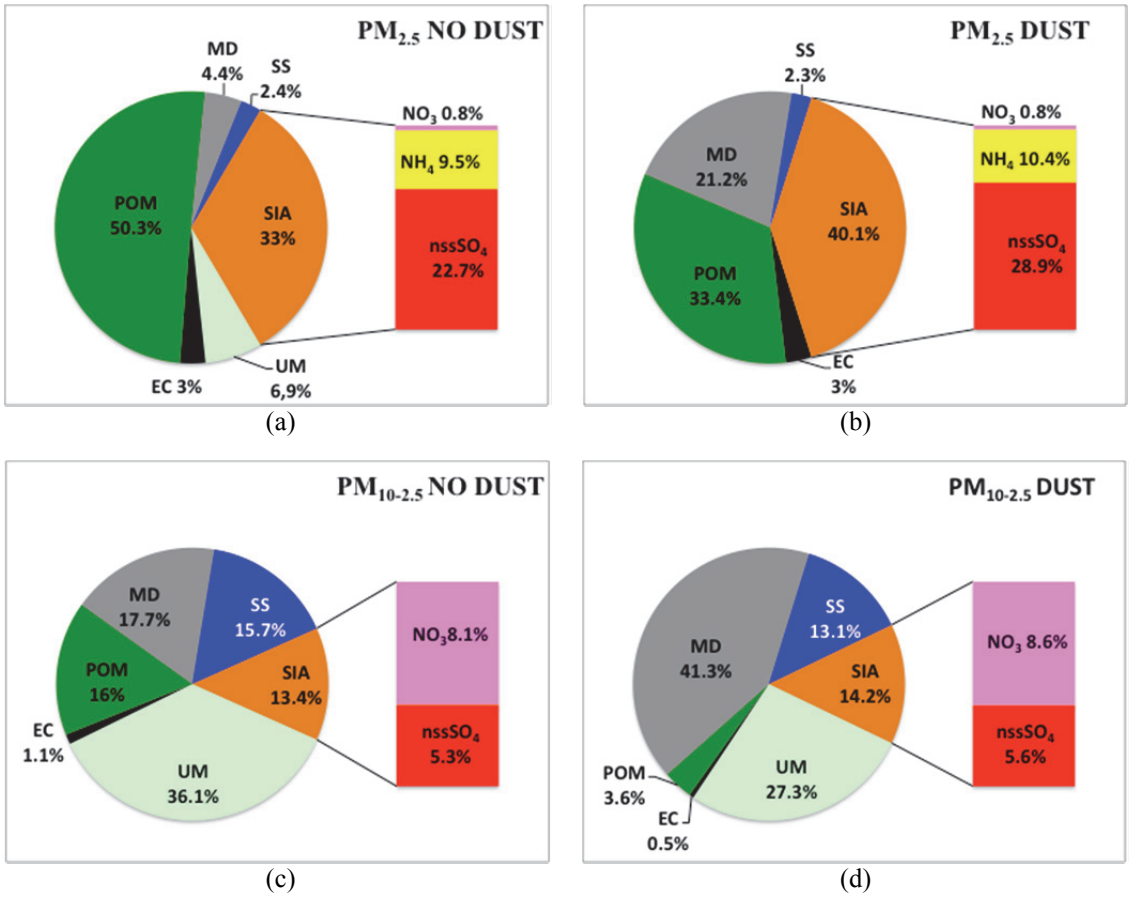

Fig. 10. Mass closure of $PM_{2.5}$ and $PM_{10–2.5}$ for non-dust (a, c) and dust (b, d) periods.

mass concentrations reveal an increase for SIA and SS in $PM_{10–2.5}$ during the dust-period, the chemical composition (Figs. 10(c) and 10(d)) showed similar relative contributions of these components during non-dust and dust periods: SIA accounted for 13.4% and 14.2% while SS accounted for 15.7% and 13.1%.

As observed for $PM_{2.5}$, during the dust transport MD contribution increased from 17.7% to 41.3% while POM decreased from 16% to 3.6%. This decrease is just the result of mass concentration increase since the POM concentrations remain similar during the whole campaign. Concerning SIA, nitrate and nss-SO_4^2 were the main components with relative contributions of 8.1 to 8.6% and 5.3 to 5.6% to $PM_{10–2.5}$ during the whole campaign.

Fig. 11 shows the linear regressions between the weighted mass and the reconstructed mass for $PM_{2.5}$ and PM_{10}, in dust and non-dust periods. This approach has been used to check the data consistency and the validity of the assumptions used for estimating particle chemical composition from measurements. Good correlations were observed for the fine fractions both for non-dust and dust periods (Figs. 11(a) and 11(b) respectively) with regression coefficients (R^2) values higher than 0.83 and slope values close to one (Table 1). The low UM percentage (< 10%) existing in non-dust period (Fig. 10) may be fully explained by the overall uncertainty associated with measurements of individual chemical components. In case of the coarse fraction, good correlation is achieved for dust period (Fig. 11(d)) since the concentrations of chemical compounds are substantially higher than in non-dust period (Table 3) and, therefore, are less affected by measurements uncertainties. However, the lack of closure (slope values 0.64 and 0.72 and UM > 27) for coarse mass fraction may be also the result of unaccounted aerosol water content which depends on the abundance of hygroscopic aerosol in the sample, errors in chemical quantification of MD, SS, POM or negative artefacts due to the volatilization of semi-volatile species from quartz and Teflon filters (Schaap *et al.*, 2004; Almeida *et al.*, 2006; Putaud *et al.*, 2010).

CONCLUSIONS

Several dust events were identified during the campaign, the highest levels of both PM_{10} and $PM_{2.5}$ concentrations observed at ground occurred between June 14th and 18th. On June 16th, PM_{10} mass concentration exceeded the European short-term (24 hour) limit value of 50 µg/m^3 requested by the EU air quality standards (Directive 2008/50/EC), the MD mass concentration was 57% of the PM_{10}.

The fine and coarse aerosol mass concentrations in dust period were two and three times higher with respect to those measured during non-dust period. The increase of fine aerosol fraction ($PM_{2.5}$) was mainly due to the increase of MD and SIA mass concentrations while the increase of

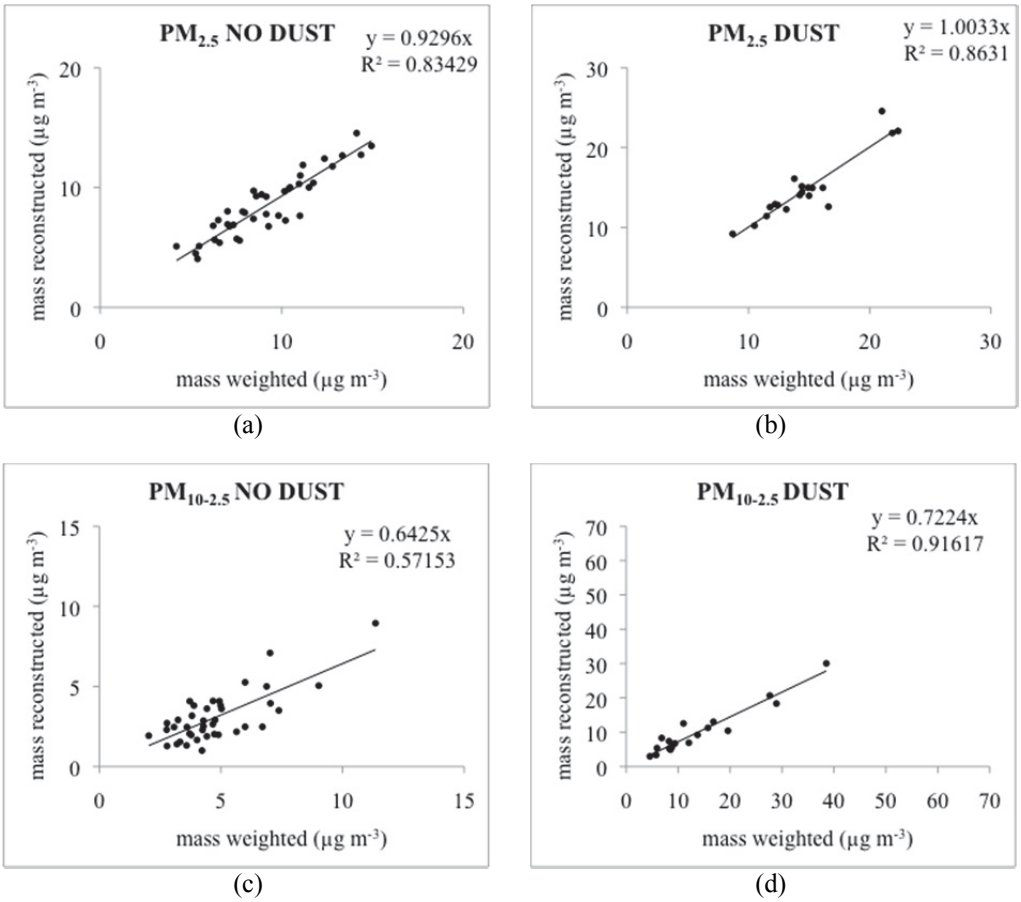

Fig. 11. Consistency between the weighted mass and the reconstructed mass of $PM_{2.5}$ and $PM_{10–2.5}$ for non-dust (40 samples) (a), (c) and dust (19 samples) (b), (d) periods.

coarse aerosol fraction ($PM_{10–2.5}$) was due to MD only. Regarding SIA, higher concentrations in dust period with respect to non-dust period were also observed for $PM_{10–2.5}$, with the difference that the major species in the $PM_{2.5}$ were NH_4^+ and $nssSO_4^{2–}$, while in $PM_{10–2.5}$ were $NO^{3–}$ and $nssSO_4^{2–}$. An increase of sea salt concentration during dust period comparing with non-dust has been also observed for both fine and coarse aerosol fractions.

POM and EC concentrations were almost unchanged by the presence of dust both in coarse and fine fractions.

ACKNOWLEDGMENTS

This work is part of the MINNI (Integrated National Model in support to the International Negotiation on Air Pollution) project, funded by the Italian Ministry of the Environment and carried out by ENEA. The authors are grateful to: D'Addiego L. and Baldassarre F. at the Trisaia Research Center for inorganic ions data, Tassinari R. at the Department of Earth Science (Ferrara University) for multi-element analysis data and Nuzzi R. at ENEA UTVALAMB-AIR lab. for carbonaceous speciation.

REFERENCES

Alastuey, A., Querol, X., Castillo, S., Escudero, M., Avila, A., Cuevas, E., Torres, C., Romero, P.M., Exposito, F., Garcia, O. and Diaz, J.P. (2005). Characterization of TSP and $PM_{2.5}$ at Izana and Sta. Cruz de Tenerife (Canary Islands, Spain) during a Saharan Dust Episode (July 2002). *Atmos. Environ.* 39: 4715–4728.

Almeida, S.M., Pio, C.A., Freitas, M.C., Reis, M.A. and Trancoso, M.A. (2006). Approaching $PM_{2.5}$ and $PM_{2.5\text{-}10}$ Source Apportionment by Mass Balance Analysis, Principal Component Analysis and Particle Size Distribution. *Sci. Total Environ.* 368: 663–674.

Aymoz, G., Jaffrezo, J.L., Jacob, V., Colomb, A. and George, Ch. (2004). Evolution of Organic and Inorganic Components of Aerosol during a Saharan Dust Episode Observed in the French Alps. *Atmos. Chem. Phys.* 4: 2499–2512.

Bougiatioti, A., Zarmpas, P., Koulouri, E., Antoniou, M., Theodosi, C., Kouvarakis, G., Saarikoski, S., Mäkelä, T., Hillamo, R. and Mihalopoulos N. (2013). Organic, Elemental and Water-soluble Organic Carbon in Size Segregated Aerosols, in the Marine Boundary Layer of the Eastern Mediterranean. *Atmos. Environ*. 64: 251–262.

Bressi, M., Sciare, J., Ghersi, V., Bonnaire, N., Nicolas, J.B., Petit, J.E., Moukhtar, S., Rosso, A., Mihalopoulos, N. and Feron, A. (2013). A One-year Comprehensive Chemical Characterization of Fine Aerosols ($PM_{2.5}$) at Urban, Suburban and Rural Background Sites in the

Region of Paris (France). *Atmos. Chem. Phys.* 13: 7825–7844.

Carbone, C., Decesari, S., Mircea, M., Giulianell, L., Finessi, E., Rinaldi, M., Fuzzi, S., Marinoni, A., Duchi, R., Perrino, C., Sargolini, T., Vardè, M., Sprovieri, F., Gobbi, G.P., Angelini, F. and Facchini, M.C. (2010). Size-resolved Aerosol Chemical Composition over the Italian Peninsula during Typical Summer and Winter Conditions. *Atmos. Environ.* 44: 5269–5278.

Cavalli, F., Viana, M., Yttri, K.E., Genberg, J. and Putaud, J.P. (2010). Toward a Standardized Thermal-optical Protocol for Measuring Atmospheric Organic and Elemental Carbon, the EUSAAR Protocol. *Atmos. Meas. Tech.* 3: 79–89.

Decesari, S., Facchini, M.C., Matta, E., Lettini, F., Mircea, M., Fuzzi, S., Tagliavini, E. and Putaud, J.P. (2001). Chemical Features and Seasonal Variation of Fine Aerosol Water-Soluble Organic Compounds in the Po Valley, Italy. *Atmos. Environ.* 35: 3691–3699.

Directive 2008/50/EC of the European Parliament and of the Council of 21 May 2008 on Ambient Air Quality and Cleaner Air For Europe. (2008). European Parliament and Council.

EC (2008). Council Directive 2008/50/EC of 21 May 2008 Relating on Ambient Air Quality and Cleaner Air for Europe. Available at: Official J. L152, 0001-0043 – http://(eur-lex.europa.eu/LexUriServ/LexUriServ.do?uri=OJ; L:2008:152:0001:0044:EN:PDF.

EC (2011). Commission Staff Working Paper Establishing Guidelines for Demonstration and Subtraction of Exceedances Attributable to Natural Sources under the Directive 2008/50/EC on Ambient Air Quality and Cleaner Air for Europe. Available at: EC Europa EU - http://ec.europa.eu/environment/air/quality/legislation/pdf/sec_2011_0208.pdf.

EN12341:1998. Determination of the PM_{10} Fraction of Suspended Particulate Matter – Reference Method and Field Test Procedure to Demonstrate Reference Equivalence of Measurement Methods EC.

EN14907:2005. Standard Gravimetric Measurement Method for the Determination of the $PM_{2.5}$ Mass Fraction of Suspended Particulate Matter.

Escudero, M., Querol, X., Pey, J., Alastuey, A., Pérez, N., Ferreira, F., Alonso, S., Rodriguez, S. and Cuevas, E. (2007). A Methodology for the Quantification of the Net African Dust Load in Air Quality Monitoring Networks. *Atmos. Environ.* 41: 5516–1691.

Flament, P., Deboudt, K., Cachier, H., Chatenet, B. and Meriaux, X. (2011). Mineral Dust and Carbonaceous Aerosols in West Africa: Source Assessment and Characterization. *Atmos. Environ.* 45: 3742–3749.

Gómez-Amo, J.L.,. Pinti, V., Di Iorio, T., di Sarra, A., Meloni, D., Becagli, S., Bellantone, V., Cacciani, M., Fuà, D. and Perrone, M.R. (2011). The June 2007 Saharan Dust Event in the Central Mediterranean: Observations and Radiative Effects in Marine, Urban, and Sub-urban Environments. *Atmos. Environ.* 45: 5385–5393.

Guinot, B., Cachier, H. and Oikonomou, K. (2007). Geochemical Perspectives from a New Aerosol Chemical Mass Closure. *Atmos. Chem. Phys.* 7: 1657–1670.

Hennigan, C.J., Bergin, M.H., Russel, A.G., Nenes, A. and Weber, R.J. (2009). Gas/Particle Partitioning of Water-soluble Organic Aerosol in Atlanta. *Atmos. Chem. Phys.* 9: 3613–3628.

Kirchstetter, T.W., Corrigan, C.E. and Novakov, T. (2001). Laboratory and Field Investigation of the Absorption of Gaseous Organic Compounds onto Quartz Filters. *Atmos. Environ.* 35: 1663–1671.

Kishcha, P., Nickovic, S., Starobinets, B., di Sarra, A., Udisti, R., Becagli, S., Sferlazzo, D., Bommarito, C. and Alpert, P. (2011). Sea-salt Aerosol Forecast Compared with Daily Measurements at the Island of Lampedusa (Central Mediterranean). *Atmos. Res.* 100: 28–35.

Kiss, G., Varga, B., Galambos, I. and Ganszky, I. (2002). Characterization of Water-soluble Organic Matter Isolated from Atmospheric Fine Aerosol. *J. Geophys. Res.* 107, doi: 10.1029/2001JD00060.

Kocak, M., Mihalopoulos, N. and Kubilay N. (2007). Contribution of Natural Sources to high PM_{10} and $PM_{2.5}$ Events in the Eastern Mediterranean. *Atmos. Environ.* 41: 3806–3818.

Kocak, M., Mihalopoulos, N. and Kubilay, N. (2007). Chemical Composition of the Fine and Coarse Fraction of Aerosols in the Northeastern Mediterranean. *Atmos. Environ.* 41: 7351–7368.

Kocak, M., Theodosi, C., Zampas, P., Séguret, M.J.M., Herut, B., Kallos, G., Mihalopoulos, N., Kubilay, N. and Nimmo, M. (2012). Influence of Mineral Dust Transport on the Chemical Composition and Physical Properties of the Eastern Mediterranean Aerosol. *Atmos. Environ.* 57: 266–277.

Kondo, Y., Miyzaki, Y., Takegawa, N., Miyakawa, T., Weber, R.J., Jimenez, L., Zhang, O. and Worsnop, D.R. (2007). Oxygenated and Water Soluble Organic Aerosols in Tokyo. *J. Geophys. Res.* 112: D01203, doi: 10.1029/2006JD007056.

Koulouri, E., Saarikoski, S., Theodosi, C., Markaki, Z., Gerasopoulos, E., Kouvarakis, G., Makela, T., Hillamo, R. and Mihalopoulos, N. (2008). Chemical Composition and Sources of Fine and Coarse Aerosol Particles in the Eastern Mediterranean. *Atmos. Environ.* 42: 6542–6550.

Malaguti, A., Mircea, M., La Torretta, T.M.G., Piersanti, A., Salvi, S., Zanini, G., Telloli, C., Salfi, F. and Berico, M. (2013). Fine Carbonaceous Aerosol Characteristics at a Coastal Rural Site in the Central Mediterranean as Given by OCEC Online Measurements. *J. Aerosol Sci.* 56: 78–87.

Malmone, F., Turpin, B.J., Solomon, P., Meng Q.Y., Robinson, A.L., Subramanian, R. and Polidori, A. (2011). Correction Methods for Organic Carbon Artifacts when Using Quartz-fiber Filters in Large Particulate Matter Monitoring Networks: The Regression Method and Other Options. *J. Air Waste Manage. Assoc.* 61: 696–710.

Marconi, M., Sferlazzo, D. M., Becagli, S., Bommarito, C., Calzolai, G., Chiari, M., di Sarra A., Ghedini, C., Gómez-Amo, J.L., Lucarelli, F., Meloni, D., Monteleone, F., Nava, S., Pace, G., Piacentino, S., Rugi, F., Severi M., Traversi, R. and Udisti, R. (2014). Saharan Dust Aerosol

over the Central Mediterranean Sea: PM_{10} Chemical Composition and Concentration versus Optical Columnar Measurements. *Atmos. Chem. Phys*. 14: 2039–2054.

Minguillòn, M.C., Querol, X., Baltensperger, U. and Prevot, A.S.H. (2012). Fine and Coarse PM Composition and Sources in Rural and Urban Sites in Switzerland: Local or Regional Pollution? *Sci. Total Environ.* 427–428: 191–202.

Miyzaki, Y., Kondo, Y., Takegawa, N., Komazaki, Y., Kawamura, M., Mochida, M., Okuzawa, K., Miyakawa, T. and Weber, R.J. (2006). Time-resolved Measurements of Water Soluble Organic Carbon in Tokyo. *J. Geophys. Res.* 111: D23206, doi: 10.1029/2006JD007125.

Nava, S, Becagli S., Calzolai, G., Chiari, M., Lucarelli, F., Prati, P., Traversi, R., Udisti, R, Valli, G. and Vecchi, R. (2012). Saharan Dust Impact in Central Italy: An Overview on Three Years Elemental Data Records. *Atmos. Environ.* 60: 444–452.

Nicolas, J.F., Galindo, N., Yubero, E., Pastor, C., Esclapez, R. and Crespo, J. (2009). Aerosol Inorganic Ions in a Semiarid Region on the Southeastern Spanish Mediterranean Coast. *Water Air Soil Pollut.* 201: 149–159, doi: 10.1007/s11270-008-9934-2.

Öztürk, F., Zararsız, A., Dutkiewicz, V.A., Husain, L., Hopke, P.K. and Tuncel, G. (2012). Temporal Variations and Sources of Eastern Mediterranean Aerosols Based on a 9-year Observation. *Atmos. Environ.* 61: 463–475.

Park, S.S. and Cho, S.Y. (2013). Characterization of Organic Aerosol Particles Observed during Asian Dust Events in Spring 2010. *Aerosol Air Qual. Res.* 13: 1019–1033.

PD CEN/TR 16243:2011. Ambient Air Quality – Guide for the Measurement of Elemental Carbon (EC) and Organic Carbon (OC) Deposited on Filters.

Pederzoli, A., Mircea, M., Finardi, S., di Sarra, A. and Zanini, G. (2010). Quantification of Saharan Dust Contribution to PM_{10} Concentrations over Italy during 2003-2005. *Atmos. Environ.* 44: 4181–4190.

Perez, N., Pey, J., Querol, X., Alastuey, A., Lopez, J.M. and Viana, M. (2008). Partitioning of Major and Trace Components in PM_{10}-$PM_{2.5}$-PM_1 at an Urban Site in Southern Europe. *Atmos. Environ.* 42: 1677–1691.

Perrino, C., Canepari, S., Catrambone, M., Dalla Torre, S., Rantica, E. and Sargolini, T. (2009). Influence of Natural Events on the Concentration and Composition of Atmospheric Particulate Matter. *Atmos. Environ.* 43: 4776–4779.

Pettijohn, F.J. (1975). Sedimentary Rocks. In *Earth Data*, NY, Harper and Row.

Pey, J., Querol, X., Alastuey, A., Forastiere, F. and Stafoggia, M. (2013). African Dust Outbreaks over the Mediterranean Basin during 2001-2011: PM_{10} Concentrations, Phenomenology and Trends, and Its Relation with Synoptic and Mesoscale Meteorology. *Atmos. Chem. Phys.* 13: 1395–1410.

Pio, C.A., Legrand, L., Oliverira, T., Afonso, J., Santos, C., Caseiro, A., Fialho, P., Barata, F., Puxbaum, H., Sanchez-Ochoa, A., Kasper-Giebl, A., Gelencser, A., Preunkert, S. and Schock, M. (2007). Climatology of Aerosol Composition (Organic versus Inorganic) at Non-urban Sites on a West-east Transect across Europe. *J. Geophys. Res.* 112: D23S02, doi: 10.1029/2006JD008038.

Putaud, J.P., Van Dingenen, R., Dell'Acqua, A., Raes, F., Matta, E., Decesari, S., Facchini, M.C. and Fuzzi, S. (2004). Size-segregated Aerosol Mass Closure and Chemical Composition in Monte Cimone (I) during MINATROC. *Atmos. Chem. Phys.* 4: 889–902.

Putaud, J.P., Van Dingenen, R., Alastuey, A., Bauer, H., Birmili, W., Cyrys, J., Flentje, H., Fuzzi, S., Gehrig, R., Hansson, H.C., Harrison, R.M., Herrmann, H., Hitzenberger, R., Huglin, C., Jones, A.M., Kasper-Giebl, A., Kiss, G., Kousa, A., Kuhlbusch, T.A.J., Loschau, G., Maenhaut, W., Molnar, A., Moreno, T., Pekkanen, J., Perrino, C., Pitz, M., Puxbaum, H., Querol, X., Rodriguez, S., Salma, I., Schwarz, J., Smolik, J., Schneider, J., Spindler, G., ten Brink, H., Tursic, J., Viana, M., Wiedensohler, A. and Raes, F. (2010). A European Aerosol Phenomenology – 3: Physical and Chemical Characteristics of Particulate Matter from 60 Rural, Urban, and Kerbside Sites across Europe. *Atmos. Environ.* 44: 1308–1320.

Querol, X., Alastuey, A., Rodriguez, S., Plana, F., Ruiz, C.R., Cots, N., Massagué, G. and Puig, O. (2001). PM_{10} and $PM_{2.5}$ Source Apportionment in the Barcelona Metropolitan Area, Catalonia, Spain. *Atmos. Environ.* 35: 6407–6419.

Querol, X., Alastuey, A., Viana, M.M., Rodriguez, S., Artinano, B., Salvador, P., Garcia do Santos, S., Patier R.F., Ruiz, C.R., de la Rosa, J., Sanchez de la Campa, A. and Menendez, M. (2004). Speciation and Origin of PM_{10} and $PM_{2.5}$ in Spain. *J. Aerosol Sci.* 35: 1151–1172.

Querol, X., Alastuey, A., Pey, J., Cusack, M., Perez, N., Mihalopulos, N., Theodosi, C., Gerasopoulos, E., Kubilay, N. and Kocak, M. (2009). Variability in Regional Background Aerosols within the Mediterranean. *Atmos. Chem. Phys.* 9: 4575–4591.

Radhi, M., Box, M.A., Box, G.P., Mitchell, R.M., Cohen, D.D., Stelcer, E. and Keywood, M.D. (2010). Size-resolved Mass and Chemical Properties of Dust Aerosols from Australia's Lake Eyre Basin. *Atmos. Environ.* 44: 3519–3528.

Remoundaki, E., Papayannis, A., Kassomenos, P., Mantas, E., Kokkalis, P. and Tsezos, M. (2013). Influence of Saharan Dust Transport Events on $PM_{2.5}$ Concentrations and Composition over Athens. *Water Air Soil Pollut.* 224: 1373, doi: 10.1007/s11270-012-1373-4.

Rinaldi, M., Emblico, L., Decesari, S., Fuzzi, S., Facchini, M.C. and Librando, V. (2007). Chemical Characterization and Source Apportionment of Size-segregated Aerosol Collected at an Urban Site in Sicily. *Water Air Soil Pollut.* 185: 311–321, doi: 10.1007/s11270-007-9455-4.

Sajani Z, Bonasoni S., Cristofanelli P., Marinoni A. and Lauriola P. (2012). Only Coarse Particles from the Sahara? *Epidemiology* 23: 642–643, doi: 10.1097/EDE.0b013e318258c23f

Salvador, P., Artinano, B., Molero, F., Viana, M., Pey, J., Alastuey, A. and Querol, X. (2012). African Dust Contribution to Ambient Aerosol Levels across Central

Spain: Characterization of Long-range Transport Episodes of Desert Dust. *Atmos. Res.* 127: 117–129, doi: 10.1016/j.atmosres.2011.12.011.

Schaap, M., Spindler, G., Schilz, M., Acker, K., Maenhaut, W., Berner, A., Wieprecht, W., Streit, N., Muller, K., Bruggemann, E., Chi, X., Putaud, J.P., Hitzenberger, R., Puxbaum, H., Baltensperger, U. and ten Brink, H. (2004). Artefacts in the Sampling of Nitrate Studied in the "INTERCOMP" Campaigns of EUROTRAC-AEROSOL. *Atmos. Environ.* 38: 6487–6496.

Sciare, J., Oikonomou, K., Cachier, H., Mihalopoulos, N., Andreae, M.O., Maenhaur, W. and Sarda-Esteve, R. (2005). Aerosol Mass Closure and Reconstruction of the Light Scattering Coefficient over the Eastern Mediterranean Sea during the MINOS Campaign. *Atmos. Chem. Phys.* 5: 2253–2265.

Seinfeld, J.H. and Pandis, S.N. (1998). *Atmospheric Chemistry and Physics. From Air Pollution to Climate Change*. New York: Wiley.

Sharma, M., Kishore, S., Tripathi, S.N. and Behera, S.N. (2007). Role of Atmospheric Ammonia in the Formation of Inorganic Secondary Particulate Matter: A Study at Kanpur, India. *J. Atmos. Chem.* 58: 1–17.

Sillanpaa, M., Hillamo, R., Saarikoski, S., Frey, A., Pennanen, A., Makkonen, U., Spolnik, Z., Van Grieken, R., Branis, M., Brunekreef, B., Chalbot, M.C., Kuhlbusch, T., Sunyer, J., Kerminen, V.M., Kulmala, M. and Salonen, R.O. (2006). Chemical Composition and Mass Closure of Particulate Matter at Six Urban Sites in Europe. *Atmos. Environ.* 40: S212–S223.

Sullivan, A.P. and Weber, R.J. (2006). Chemical Characterization of the Ambient Organic Aerosol Soluble in Water Part 2: Isolation of Acid, Neutral and Basic Fractions by Modified Size Exclusion Chromatography. *J. Geophys. Res.* 111: D05315, doi: 10.1029/2005JD006486.

Sullivan, A.P., Peltier, R.E., Brock, C.A., de Gouw, J.A., Holloway, J.S., Warneke, C., Wollny, A.G. and Weber, R.J. (2006). Airborne Measurements of Carbonaceous Aerosol Soluble in Water over Northeastern United States: Method Development and Investigation into Water-soluble Organic Carbon Sources. *J. Geophys. Res.* 111: D05314, doi: 10.1029/2005JD006485.

Theodosi, C., Grivas, G., Zarmpas, P., Chaloulakou, A. and Mihalopoulos, N. (2011). Mass and Chemical Composition of Size-segregated Aerosols (PM_1, $PM_{2.5}$, PM_{10}) over Athens, Greece: Local versus Regional Sources. *Atmos. Chem. Phys.* 11: 11895–11911.

Theodosi, C., Im, U., Bougiatioti, A., Zampas, P., Yenigun, O. and Mihalopoulos, N. (2010). Aerosol Chemical Composition over Istanbul. *Sci. Total Environ.* 408: 2482–2491.

Turpin, B.J. and Lim, H.J. (2001). Species Contributions to $PM_{2.5}$ Mass Concentrations: Revisiting Common Assumptions for Estimating Organic Mass. *Aerosol Sci. Technol.* 35: 602–610.

Viana, M., Chi, X., Maenhaut, W., Querol, X., Alastuey, P., Mikuska, P. and Vecera, Z. (2006). Organic and Elemental Carbon Concentrations in Carbonaceous Aerosols during Summer and Winter Sampling Campaigns in Barcelona, Spain. *Atmos. Environ.* 40: 2180–2193.

Viana, M., Kuhlbusch, T.A.J., Querol, X., Alastuey, P., Harrison, R.M., Hopke, P.K., Winiwarter, W., Vallius, M., Szidat, S., Prevot, A.S.H., Hueglin, C., Bloemen, H., Wahlin, P., Vecchi, R., Miranda, A.I., Kasper-Giebl, A., Maenhaut, W. and Hitzenberger, R. (2008). Source Apportionment of Particulate Matter in Europe: A Review of Methods and Results. *J. Aerosol Sci.* 39: 827–849.

Weber, R.J., Sullivan, A.P., Peltier, R.E., Russel, A., Yan, B., Zheng, M., De Gouw, J., Warneke, C., Brock, C., Holloway, J.S., Atlas, E.L. and Edgerton, E. (2007). A Study of Secondary Organic Aerosol Formation in the Anthropogenic-influenced Southeastern United States. *J. Geophys. Res.* 112: DI3302, doi: 10.1029/2007JD008408.

Received for review, August 20, 2014
Revised, December 3, 2014
Accepted, December 22, 2014